



FIRST-Nuclides

(Contract Number: **295722**)

DELIVERABLE (D-N°:4.1)

STATUS OF MODELLING OF MIGRATION/RETENTION PROCESSES OF FISSION PRODUCTS IN THE SPENT FUEL STRUCTURE

Author(s): **Ignasi Casas and Joan de Pablo**

Reporting period: e.g. **01/01/2012 – 30/06/2013**

Date of issue of this report: **05/05/2013**

Start date of project : **01/01/2012**

Duration : **36 Months**

Project co-funded by the European Commission under the Seventh Euratom Framework Programme for Nuclear Research & Training Activities (2007-2011)		
Dissemination Level		
PU	Public	X
RE	Restricted to a group specified by the partners of the [FIRST-Nuclides] project	
CO	Confidential, only for partners of the [FIRST-Nuclides] project	

(D-N°: 4.1) – STATUS OF MODELLING OF MIGRATION/RETENTION PROCESSES OF FISSION PRODUCTS IN THE SPENT FUEL STRUCTURE

Dissemination level: **PU**

Date of issue of this report: **5/5/2013**



DISTRIBUTION LIST

Name	Number of copies	Comments
Mr. Christophe Davies (European Commission)	One electronic copy submitted via participant portal	
All consortium members and European Commission	One electronic copy available on the FIRST-Nuclides webportal	

(D-N°: 4.1) – STATUS OF MODELLING OF MIGRATION/RETENTION PROCESSES OF FISSION PRODUCTS IN THE SPENT FUEL STRUCTURE

Dissemination level: [PU](#)

Date of issue of this report: [5/5/2013](#)



INDEX

ABSTRACT	4
1. INTRODUCTION	4
2. CHEMICAL COMPOSITION	5
3. CHEMICAL STATE	7
4. CHEMICAL COMPOUNDS	11
5. LOCALIZATION OF FISSION PRODUCTS IN THE FUEL	14
6. MODELLING MIGRATION/RETENTION PROCESSES	16
7. CONCLUSIONS	20
8. REFERENCES	21

(D-N°: 4.1) – STATUS OF MODELLING OF MIGRATION/RETENTION PROCESSES OF FISSION PRODUCTS IN THE SPENT FUEL STRUCTURE

Dissemination level: [PU](#)

Date of issue of this report: [5/5/2013](#)



ABSTRACT

This report gives an overview of the chemical composition of the fission products in irradiated UO₂ fuels. Special attention has been made in their chemical state and the chemical compounds formed in reactor operation. Localization of fission products in different parts of the fuel such as gap, rim, grain boundary and grain is also discussed. Finally, migration and retention processes in the fuel structure can be modeled by using different approaches, empirical models which correlate fission gas release with the release of other radionuclides; thermodynamic models based on phase diagrams and thermochemistry; and mechanistic models which consider intragranular fission product transport from the bulk to the grain boundary, accompanied by both formation of precipitates and gaseous species in the intergranular bubbles.

1. INTRODUCTION

Performance assessment (PA) of the final spent fuel disposal requires a definition of the source term, this term is usually described as the combination of both radionuclides release instantaneously and radionuclides released congruently with the matrix dissolution process. The so called, instant release fraction (IRF) represents the fraction of the inventory of safety-relevant radionuclides that may be rapidly released from the fuel and fuel assembly at the time of canister breach [Johnson et al. 2005]. PA exercises considered the IRF to be the main source of radiological risk in geological disposal.

In spent fuel leaching experiments, the problem is how to establish a leaching time to determine IRF. Currently this time is arbitrary, for example in [Serrano-Purroy et al. 2012] IRF was calculated at 10 days while Roudil et al. [2007] established this time at 60 days. In both works, the release of selected radionuclides followed after more than one year of leaching time but a lower rate.

Probably, an important process in IRF is related to water contact to the different parts of the fuel but also which is the chemical state and location of the fission products.

In this contribution a review of migration and retention processes of fission products in the structure of the spent fuel is given. This will be focused in radionuclides different from fission gases since these have been discussed in detail in Deliverable D-

Nº: 4.2 (2013). Fission gas release modeling has been investigated for a long time and it is well understood.

2. CHEMICAL COMPOSITION

The chemical composition evolution in the spent fuel during irradiation is due to the following processes:

- a) Uranium decrease content due to the fission processes.
- b) Neutron capture processes to produce different Uranium and Plutonium isotopes; and minors actinides such as Americium, Neptunium and Curium.
- c) Production of many fission products.

Actinides and Fission Products inventory during irradiation can be calculated by using neutronic calculations codes. Different institutions apply different codes, in France reported inventories are normally calculated by CESAR5; in Germany the most used code is the KORIGEN which is based on the Oak Ridge Isotope Generation and Depletion code ORIGEN. The ORIGEN-ARP code is generally used in the inventory calculations of Spanish nuclear fuels.

Data obtained by using different codes indicates no important differences between them. As an example, CESAR and ORIGEN2 results are compared in Table 1.

Table 1. Inventory comparison (in terms of fraction) obtained by [POINSSOT, C. et al., 2001] using the CESAR code and those obtained by [KUROSAKI, K. et al., 1999] using the ORIGEN-2 code

Elements (%)	ORIGEN-2	CESAR
Uranium	0.881	0.92
Plutonium	0.011	0.013
Zr + Nb	0.014	0.016
Mo + Tc	0.013	0.018
Pt group	0.019	0.018
Cd + Sn	$8 \cdot 10^{-4}$	$6.25 \cdot 10^{-4}$
Te + Se + Sb	$1.7 \cdot 10^{-3}$	$1.91 \cdot 10^{-3}$

Elements (%)	ORIGEN-2	CESAR
I + Br	$8 \cdot 10^{-4}$	$8 \cdot 10^{-4}$
Cs + Rb	$8.8 \cdot 10^{-3}$	0.010
Alkaline earth	$7.4 \cdot 10^{-3}$	$8.8 \cdot 10^{-3}$
Rare earth	0.027	0.037

The reliability of these calculations can be compared to experimental inventory determination. Recently [Gonzalez-Robles, E., 2012], this comparison was carried out for a PWR fuel pellet with a burn-up of 52 MWd/kgU (cooling time 6 years), results are shown in Table 2.

Table 2. Comparison between experimental and calculated element determination ($\mu\text{g}_{\text{element}}/\text{g}_{\text{SNF}}$) in a 52 MWd/kgU PWR UO₂ fuel.

Element	52BU experimental	52BU theoretical (ORIGEN-ARP)
Rb	640 ± 130	500
Sr	2180 ± 440	1190
Y	800 ± 200	660
Zr	7600 ± 1500	5100
Mo	4400 ± 900	4700
Tc	1200 ± 250	1100
Ru	4100 ± 800	2900
Rh	800 ± 200	600
Cs	4700 ± 200	3500
Ba	3500 ± 700	2300
La	2100 ± 400	1700
Nd	7000 ± 1400	5500
U	870000 ± 87000	823000
Np	1200 ± 300	700
Pu	7300 ± 1500	9700
Am	1100 ± 200	400
Cm	140 ± 30	60

The values obtained during the experimental determination of the inventory for 52BU nuclear fuel taking the uncertainties into account were in the same range as the theoretical values. The exceptions were Ba, Pu, Am and Cm, as it can be seen in Figure 1. In spite of these discrepancies, it is clear that theoretical calculations are good enough to be used when experimental determinations are not available, even for burn-ups higher than 40 MWd/kgU.

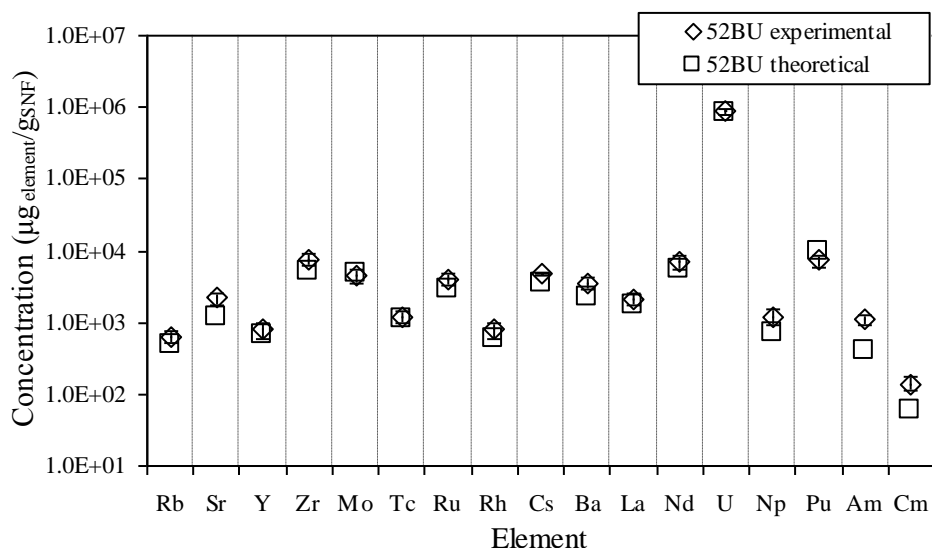


Figure 1. Comparison of concentration ($\mu\text{g}_{\text{element}}/\text{g}_{\text{SNF}}$) from experimental and theoretical determinations, for 52BU Nuclear Fuel.

3. CHEMICAL STATE

Classification of the chemical state of the fission products (FP) was carried by Kleykamp [1985], he divided them into four groups:

- 1) Fission gases and other volatile FP
- 2) Fission products forming metallic precipitates
- 3) Fission products forming oxide precipitates
- 4) Fission products dissolved as oxides in the fuel matrix

FP chemical state depends basically on the relative partial molar Gibbs free energy of oxygen. At the conditions of UO_2 fuel sintering, the oxygen potential is around -450 kJ/mol, this value is more or less constant as a function of the reactor temperature as

it is discussed by Matzke (1995) for fuels for medium burn-up (34.5 MWd/kgU). This value is similar to the oxygen potential of the Mo/MoO₂ equilibrium indicating that this fission product could play the role of oxygen buffer; in Matzke (1994) this role is studied, observing that several fuel compositions have lower oxygen potential than the couple Mo/MoO₂ at 750°C.

To understand the continuous transitions between metallic and oxide precipitates due to similar oxygen potentials and the fuel which changes its composition during irradiation and fission product formation is very helpful the use of Ellingham diagrams as shown in Figure 2 [Kleykamp, 1985].

As it can be seen in Figure 2, fission products with Gibbs free energies (ΔG°) lower than the oxygen potential of the different fuel composition (UO_{2+x} and U_{0.8}Pu_{0.2}O_{2±x}) are present in fuel as oxide precipitates. On the contrary, if ΔG° is higher, then fission products forms metallic precipitates.

Regarding the fission products dissolved in the fuel matrix, cesium, barium and tellurium are soluble in the fuel in small quantities [Kleykamp, 1985; Sari et al., 1979]. Strontium, zirconium and niobium are, in some extent, soluble [Kleykamp, 1985] whereas large solubilities are observed for rare earth elements in UO₂ fuels in both UO₂-ReO₂ and UO₂-Re₂O₃ systems.

For high burn-up fuels, six different groups of elements can be considered as constituents of spent fuels [Ferry et al. 2005]. Taking into account the mass fraction of each group, the following order can be established:

- 1) Actinides
- 2) Lanthanides
- 3) Metallic precipitates
- 4) Oxides precipitates
- 5) Gases and volatiles
- 6) Metalloids

The most important elements, for the different groups mentioned above, present in the UO₂ fuel can be seen in Figure 3, a detail description of the chemical compounds formed during irradiation is commented below (see 4.).

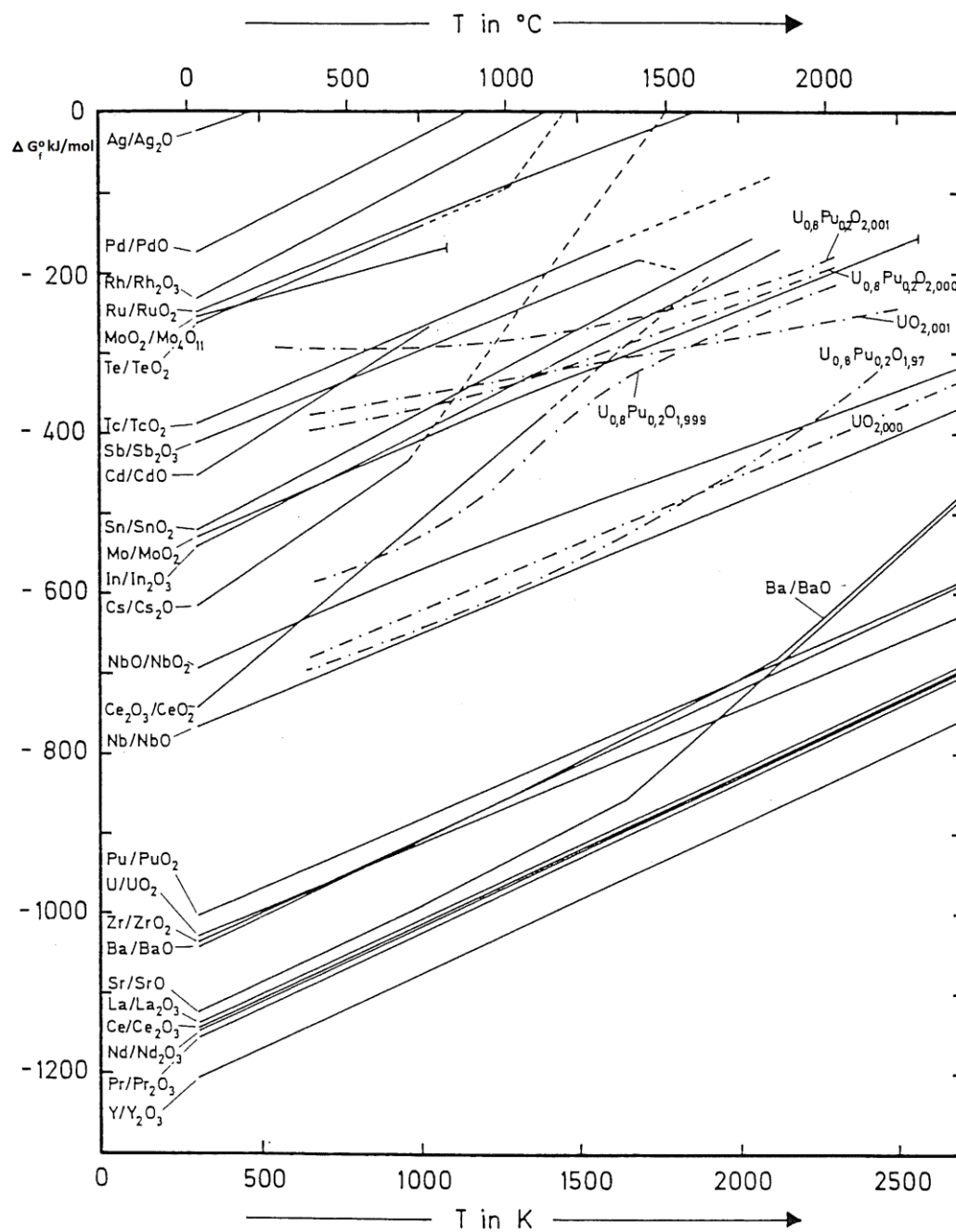


Figure 2. Gibbs free energy (ΔG°) of fission products and UO_{2+x} and $U_{0.8}Pu_{0.2}O_{2+x}$

(D-N°: 4.1) – STATUS OF MODELLING OF MIGRATION/RETENTION PROCESSES OF FISSION PRODUCTS IN THE SPENT FUEL STRUCTURE

Dissemination level: PU

Date of issue of this report: 5/5/2013



PERIODIC TABLE OF THE MAIN ELEMENTS PRESENT IN THE IRRADIATED URANIUM DIOXIDE FUEL																															
1 Hydrogen 1.0079 H																	18 Helium 4.0026 He														
2 Lithium 6.941 Li	3 Sodium 22.9898 Na	4 Potassium 39.0983 K	5 Rubidium 85.468 Rb	6 Cesium 132.905 Cs	7 Francium (223) Fr	8 Beryllium 9.0122 Be	9 Magnesium 24.3050 Mg	10 Calcium 40.078 Ca	11 Strontium 87.62 Sr	12 Barium 137.327 Ba	13 Radium 226.025 Ra	14 Boron 10.811 B	15 Carbon 12.011 C	16 Nitrogen 14.0067 N	17 Oxygen 15.9994 O	18 Fluorine 18.9984 F	19 Neon 20.1797 Ne														
19 Rubidium 85.468 Rb	20 Cesium 132.905 Cs	21 Francium (223) Fr	22 Scandium 44.9559 Sc	23 Titanium 47.88 Ti	24 Vanadium 50.9415 V	25 Chromium 51.9961 Cr	26 Manganese 54.9380 Mn	27 Iron 55.847 Fe	28 Cobalt 58.9332 Co	29 Nickel 58.693 Ni	30 Copper 63.546 Cu	31 Zinc 65.39 Zn	32 Gallium 69.723 Ga	33 Germanium 72.61 Ge	34 Arsenic 74.9216 As	35 Selenium 78.96 Se	36 Bromine 79.904 Br	37 Krypton 83.84 Kr													
37 Rubidium 85.468 Rb	38 Cesium 132.905 Cs	39 Francium (223) Fr	40 Strontium 87.62 Sr	41 Yttrium 88.9058 Y	42 Zirconium 91.224 Zr	43 Niobium 92.9063 Nb	44 Molybdenum 95.94 Mo	45 Technetium (98) Tc	46 Ruthenium 101.07 Ru	47 Rhodium 101.07 Rh	48 Palladium 106.367 Pd	49 Silver 107.868 Ag	50 Cadmium 112.411 Cd	51 Indium 114.818 In	52 Tin 118.710 Sn	53 Antimony 121.757 Sb	54 Tellurium 127.60 Te	55 Iodine 126.905 I	56 Xenon 131.29 Xe												
55 Rubidium 85.468 Rb	56 Cesium 132.905 Cs	57 Francium (223) Fr	58 Strontium 87.62 Sr	59 Yttrium 88.9058 Y	60 Zirconium 91.224 Zr	61 Niobium 92.9063 Nb	62 Molybdenum 95.94 Mo	63 Technetium (98) Tc	64 Ruthenium 101.07 Ru	65 Rhodium 101.07 Rh	66 Palladium 106.367 Pd	67 Silver 107.868 Ag	68 Cadmium 112.411 Cd	69 Indium 114.818 In	70 Tin 118.710 Sn	71 Antimony 121.757 Sb	72 Tellurium 127.60 Te	73 Iodine 126.905 I	74 Xenon 131.29 Xe												
87 Francium (223) Fr	88 Radium 226.025 Ra	89 Actinium 227.028 Ac	90 Thorium 232.0377 Th	91 Protactinium 231.03688 Pa	92 Uranium 238.02891 U	93 Neptunium 237.048173 Np	94 Plutonium 244.0642 Pu	95 Americium 243.06136 Am	96 Curium 247.070352 Cm	97 Berkelium 247.070352 Bk	98 Californium 251.079589 Cf	99 Einsteinium 252.0833 Es	100 Fermium 257 Fm	101 Mendelevium 258 Md	102 Nobelium 259 No	103 Lawrencium 260 Lr	104 Rutherfordium 261 Rf	105 Dubnium 262 Db	106 Seaborgium 263 Sg	107 Bohrium 264 Bh	108 Hassium 265 Hs	109 Meitnerium 266 Mt	110 Darmstadtium 267 Dt	111 Roentgenium 268 Rg	112 Copernicium 269 Cn	113 Nihonium 270 Nh	114 Flerovium 271 Fl	115 Moscovium 272 Mc	116 Livermorium 273 Lv	117 Tennessine 274 Ts	118 Oganesson 276 Og

Figure 3. Main elements present in high burn-up UO_2 fuels.

The mass fraction of each group calculated for a fuel with a burn-up of 60 MWd/kgU after 50 years' cooling time is shown in Table 3 (Ferry et al. 2005).

Table 3. Mass distribution for a UO_2 fuel (60 MWd/kgU) after 50 years' cooling time.

	mass (%)
ACTINIDES	93.780
LANTHANIDES	1.860
METALLIC PRECIPITATES	1.679
OXIDE PRECIPITATES	1.606
GAS & VOLATILES	1.063
METALLOIDS	0.00961

(D-N°: 4.1) – STATUS OF MODELLING OF MIGRATION/RETENTION PROCESSES OF FISSION PRODUCTS IN THE SPENT FUEL STRUCTURE

Dissemination level: PU

Date of issue of this report: 5/5/2013



4. CHEMICAL COMPOUNDS

The knowledge of the chemical compounds in the spent fuel can be important in order to understand the radionuclide release when water contacts the fuel. As discussed above, main compounds are oxides and metallic precipitates, however other types of compounds have been detected in UO₂ fuels.

The behavior of fission gases formed during irradiation are discussed in the frame of the First Nuclide project elsewhere [Pekala et al. 2013].

4.1. Cesium

The chemistry of both cesium and rubidium in UO₂ fuels is very important because they react with the matrix, with cladding components and with other fission products leading to swelling and cladding corrosion at high oxygen potentials.

Based on thermodynamic equilibrium and solubility studies of cesium in UO₂, part of this fission product can be found as (U,Pu,Cs,FP)O_{2-x} oxides, such as Cs₂(U,Pu)₄O₁₂ or Cs₂(U,Pu)O₄ [Kleykamp, 1985].

In general, the existence of Cs₂M₄O₁₂ in equilibrium with MO₂ and liquid Cs was proven, where M=U_{0.8}Pu_{0.2} while the formation of Cs₂(U,Pu)O₄ has not been proven in irradiated UO₂ fuels.

Reactions with other FP give the following compounds: Cs₂MoO₄ [Imoto, 1986; Kurosaki et al., 1999; Dehaut, 2000]; Cs₃Te₂ [Dehaut, 2000]; Cs₂Te [Imoto, 1986; Kurosaki et al., 1999] and CsI [Kurosaki et al., 1999; Dehaut, 2000].

4.2. Iodine

Iodine chemical state within the fuel is not completely clear. It is reported that iodine release from UO₂ tends to surpass that of Xe at temperatures above 300°C, however chemical models predict a fractional release rate of iodine orders of magnitude below that of the fission gases, since models indicate that iodine exists in a less volatile chemical state, for example CsI [Kleykamp, 1985].

The formation of CsI in the spent fuel is already controversial, CsI traces were detected in parts of the pellets with temperatures around 500°C inside the cladding [Kleykamp, 1985]. By using microstructural analysis of UO₂ fuels with burn-ups from 44 to 48 MWd/kgU, it was not possible to detect CsI [Thomas et al., 1992]. Moreover

radial analysis of both radionuclides indicates that iodine migrates slightly faster than cesium which contradicts an excessive CsI formation during distribution [Peehs et al. 1981].

4.3. Selenium and Tellurium

In spite of Selenium has been considered relevant in the safety analysis of the final spent fuel disposal, no data of selenium compounds in the fuel has been described. Taking into account thermodynamic equilibrium calculations, Cs₂Se has been proposed [Cubbicciotti & Sanecki, 1978], with similar properties to CsI.

Thermodynamic equilibrium calculations indicate that Tellurium should be forming Cs₂Te and Cs₃Te₂ [Dehaut et al. 2000]. However, Cs₂Te has never been detected [Thomas, 1992].

The oxygen potential of the Te/TeO₂ equilibrium is higher than that of LWR oxides, see Figure 2. Therefore, Tellurium can form metallic phases (with U, Pd, Sn), can be a constituent of multi-component fuel-fission oxides (Cs-Ba-U-Pu-O-Te) and can be dissolved in the oxide fuel (U-Pu,Te,FP)O_{2-x} [Kleykamp, 1985].

Some recent results by using the Knudsen cell seem to indicate that a fraction of Tellurium is released at a temperature lower than 1500°C [Serrano-Purroy, personal communication].

4.4. Molybdenum, Technetium, Ruthenium, Rhodium and Palladium

These five elements are the components of the so-called “white inclusions” which corresponds to metallic precipitates, these phases are mostly hexagonal. The composition of this phase is given in Table 4.

Table 4. Metallic precipitate composition

Mo	Ru	Tc	Rh	Pd	
55-60	26-32	12	5-6	2-4	(Kohli, 1987)
35	30	10	5	20	(Thomas et al., 1992)

As it can be observed, Mo and Ru are the main components of the metallic phases within the fuel. Pd is one of the fission products which forms compounds with many FPs, from both the fuel and the cladding. Phases such as Pd-Ag-Cd and Pu(Pd, In, Sn, Te) [Thomas, 1992; Kleykamp, 1985].

4.5. Strontium and Barium

Strontium oxide is predominantly dissolved in UO_2 and $(\text{U,Pu})\text{O}_2$, for this reason some authors proposed Sr as indicator of the spent fuel matrix dissolution [xxx]. However, some discrepancies have been observed in leaching experiments where Sr is released 3-4 times faster than uranium.

In the case of Barium, only a smaller fraction of the oxide forms solid solution with the fuel. Barium forms BaUO_3 and BaZrO_3 in fuel, BaZrO_3 can incorporate small quantities of several radionuclides such as Sr, Cs, U, Pu, Mo and REE, the following precipitate has been proposed $(\text{BaCs,Sr})(\text{U,Pu,Zr,Mo,REE})\text{O}_3$ [Kleykamp, 1985].

4.6. Zirconium

Zirconium oxide is completely miscible with PuO_2 [Carroll, 1963]. The solubility in UO_2 is restricted and is strongly dependent on temperature (50% at 1700°C), as it was mentioned above Zr forms the BaZrO_3 perovskite structure [Kleykamp, 1985].

4.7. Lanthanides

La, Ce, Pr, Nd, Pm, Sm and Eu oxides are very soluble in UO_2 . At high burn-ups, small fractions of the REE can be found in the perovskite oxide phases.

Recently, Dehaut et al. (2000) gave the compound percentage for several FP, these results are collected in Table 5 for a spent fuel with a burn-up of 60 MWd/kgU.

Table 5. Compound percentage for several fission products

Characteristics of the UO_2 fuel	Burn-up= 60 MWd/kgU O/M=1.997 $\Delta G^\circ(\text{O}_2) = -420 \text{ kJ/mol}$ T = 750°C
Fission products	
Mo	48 % Mo, 34 % MoO_2 (ss), 18 % Cs_2MoO_4
Cs	58 % Cs_2MoO_4 , 32 % Cs_3Te_2 , 10 % CsI

Te	100 % Cs ₃ Te ₂
Ba	100% BaZrO ₃
Zr	51 % BaZrO ₃ , 49 % ZrO ₂ (ss)
I	100 % CsI

5. LOCALIZATION OF FISSION PRODUCTS IN THE FUEL

The location of radionuclides in the irradiated fuel depends on mechanisms and migration kinetics during operation. Fission gas release mechanism has been studied in detail, a summary of these studies are collected in Deliverable (D-N^o:4.2) (*Models for fission products release from spent nuclear fuel and their applicability to the First Nuclides project*).

Diffusion is the main mechanism responsible for the mobility of fission products. It is possible to distinguish three areas of different behavior in the reactor as a function of the temperature [Matzke, 1983]:

- Below 1000°C, diffusion coefficient is independent on T, mobility seems to be due to fission reactions.
- Between 1000°C and 1600°C, diffusion is mixed, it depends on both Temperature and fission reactions.
- Above 1600°C, diffusion depends on temperature.

Diffusion studies were carried out in detail by Matzke [1983, 1987, 1990].

The mobility of FPs in the fuel by the effect of temperature depends on the chemical properties of the element such as electronegativity and ion size, for example a cation forming a solid solution with the UO₂ is much less mobile than an interstitial neutral atom [Prussin, 1988]. Electronegativity elements non soluble in UO₂ as I and Te are released at higher rates than weak electronegativity elements as Cs and Ba.

FP diffusion due to irradiation has been observed in the reactor, and it is the responsible of the radionuclide mobility for temperatures below 800°C, which is the case of the periphery of the pellet.

FP migrate by diffusion to the different parts of the fuel due to changes of morphology during operation. It is possible to differentiate the following parts:

- a) Free volumes such as bubbles, cracks and the gap.
- b) Restructured zone, the increase of the burn-up, due to neutron capture of U-238 to produce Pu-239, generates an external layer on the fuel with a higher burn-up, increased porosity and fuel grain subdivision, which results on the formation of the so-called rim or High Burn-Up Structure (HBS) [Hiernaut et al., 2008], which is observed at BU's higher than 40 MWd/kgU. The increase of BU can produce the contact between the pellet and the cladding by swelling and consequently, closing the gap.
- c) Grain boundaries of the non restructured matrix, gases and volatiles can be easily released from them due to temperature transitions or fuel oxidation.
- d) Grains, the so-called UO₂ fuel matrix.

From different studies [Ferry et al., 2004; Johnson & Tait, 1997; Johnson & McGinnes, 2002] a good summary of FP's location in UO₂ fuel can be found in [Johnson et al., 2004], results are collected in Table 6.

Table 6. Distribution of Radionuclides in the different parts of the fuel

Components	Radionuclides
Gap	Fission gases, volatiles: ¹²⁹ I, ¹³⁷ Cs, ¹³⁵ Cs, ⁷⁹ Se, ¹²⁶ Sn
Rim porosity	Fission gases, volatiles: ¹²⁹ I, ¹³⁷ Cs, ¹³⁵ Cs, ⁷⁹ Se, ¹²⁶ Sn, Sr
Rim grains	Actinides, FP
Grain boundaries	Fission gases, volatiles: ¹²⁹ I, ¹³⁷ Cs, ¹³⁵ Cs, ⁷⁹ Se, ¹²⁶ Sn, segretated metals: ⁹⁹ Tc, ¹⁰⁷ Pd
Grains	Actinides, remaining FPs and activation products

In Figure 4, a summary of the the location of radionuclides together with chemical compounds formed in the fuel can be observed.

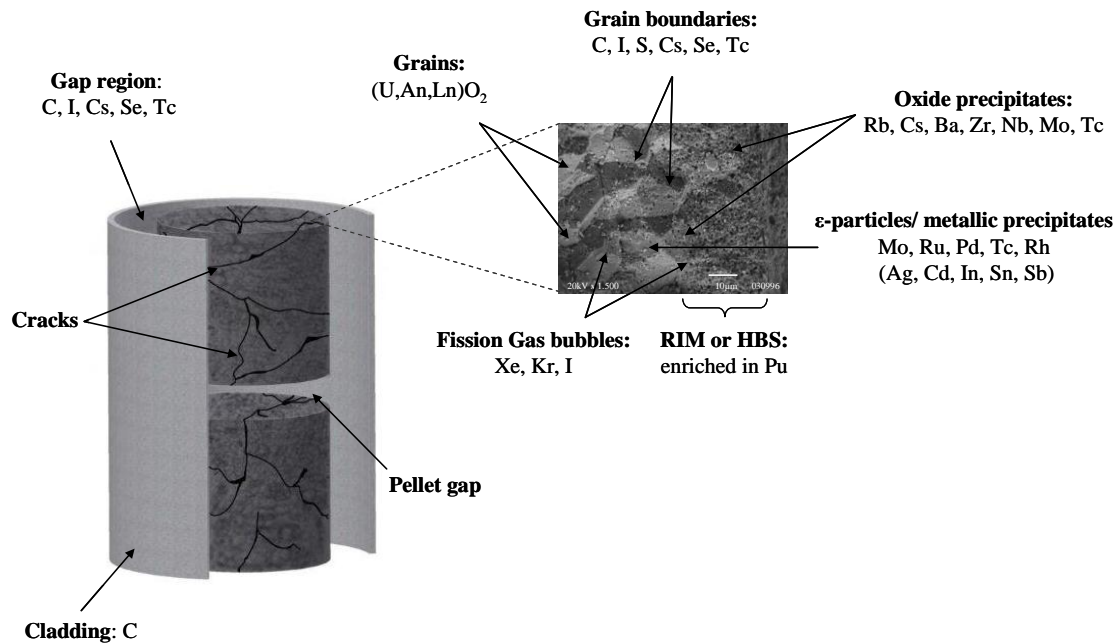


Figure 4. Chemical composition and localization of the radionuclides in the UO_2 fuel

6. MODELLING MIGRATION/RETENTION PROCESSES

Fission gas migration and modelling is discussed in detail in Deliverable (D-N^o:4.2) (*Models for fission products release from spent nuclear fuel and their applicability to the First Nuclides project*) and references therein. A great number of fuel performance codes are available to predict the behaviour of a reactor rod during both normal and abnormal operation in the nuclear reactor. Capabilities of TRANSURANUS code were recently presented by Van Uffelen [2012], showing the combination of different aspects of the fuel in the reactor: thermal analysis; mechanical analysis; fission gas generation, transport and release; thermal and irradiation induced densification of the fuel; volume changes due to phase changes and neutronics.

6.1. Empirical Modeling

This model is based on establishing correlations between fission gas release (FGR) and other fission products normally the so-called volatiles such as iodine and cesium. In the case of ^{137}Cs , a correlation with FGR equal to 1:3 has been found for FGR values higher than 1%, analyzing experimental results only a few experiments corroborate this correlation. Some authors [nagra] pointed out that this finding is consistent with

the fact that diffusion coefficient of Cs in the fuel is lower than that of FG [Poinssot et al. 2001]. No explanation is given in order to explain the similar release when FGR is around 1%.

In the case of ^{129}I , the correlation with the FGR was suggested to be 1:1 [Gray, 1999]. This agrees with the observation of both iodine and xenon have similar diffusion coefficient in the fuel [Poinssot et al. 2001]. The major part of the iodine seems to be located in the grain boundaries, in contrast to cesium which is located in the gap. Recently, Johnson et al. [2012] have provided new data on short-term release of ^{137}Cs and ^{129}I for a number of fuels irradiated to burn-ups of 50–75 MWd/kgU. The results show that the fractional release of ^{137}Cs is usually much lower than the FGR. Fractional ^{129}I releases are somewhat larger, but only when the fuel was extracted from the cladding.

The different behaviour of ^{129}I and ^{137}Cs is also contradictory if CsI is considered the main compound formed in the fuel.

No other empirical correlation with FGR has been proposed for other fission products.

6.2. Thermodynamic Models

These models are based on the assessment of Gibbs energy parameters for the individual phases as functions of temperature, composition and pressure. For the more of 30 years, the CALPHAD (Computer Coupling of Phase Diagrams and Thermochemistry) method has demonstrated to be a useful tool for solving problems in the field of materials and thermochemistry.

In Table 7, selected software is shown [Schmid-Fetzer et al., 2007] for thermodynamic and phase diagram calculations. Different capabilities are included in most software, for example several types of calculations: point calculation, line calculation, two-dimensional section, liquidus projection and Scheil solidification simulation. Phase models such as substitutional solution, gas molecules and stoichiometric compounds are also included.

Table 7. Selected software* for thermodynamic and phase diagram calculations

FactSage	www.factsage.com
TDATA	www.npl.co.uk/data
Pandat; WinPhad	www.computherm.com
Thermo-Calc	www.thermocalc.com
Thermosuite	www.thermodata.free.fr

*Discussed in detail in the special issue of CALPHAD 26 (2002)

Specific Database for a number of compounds of reactor materials and fission products is the so-called NUCLEA [2007] which is a thermodynamic database for in and ex-vessel applications containing 18 + 2 elements:

O-U-Zr-Ag-In-B-C-Fe-Cr-Ni-Ba-La-Sr-Ru-Al-Ca-Mg-Si + Ar-H

and including the 15 oxide system :

UO₂-ZrO₂-In₂O₃-B₂O₃-FeO-Fe₂O₃-Cr₂O₃-NiO-BaO-La₂O₃-SrO-Al₂O₃-CaO-MgO-SiO₂

Quality of thermodynamic data has been determined by comparison between calculation and available experimental data. In NUCLEA data, four different categories have been established:

- Estimated: No experimental data available
- Perfectible: Some domains need more experimental information
- Acceptable: The system is known and satisfactorily modeled
- High quality: The system is quite well known and modeled

6.3. Mechanistic Models

Advanced mechanistic codes in order to describe FGR and fuel swelling as a function of fuel fabrication and in a wide range of reactor operation are FASTGRASS [Rest and Zawadki, 1994] and VICTORIA [Heames et al., 1992]. Both are essentially

based on consideration of the equilibrium state of the bubbles, this is a simplification since defect structure of the crystal is almost completely excluded.

Recently, to avoid these problems the development of the code module for FP release (MFPR) has been carried out [Veshchunov et al., 2006].

The code considers that the most important FPs created in the fuel matrix are the following: Cs, Ce, I, Eu, Mo, Nd, Ru, Nb, Ba, Ss, Sr, Te, Zr, Xe and La and assumes that all these elements are in the matrix in atomic form. All impurity atoms formed due to fission processes migrate to grain boundaries. In this way, fission-gas atoms can be captured by intragranular gas bubbles, which can also migrate to grain boundaries. Part of the captured atoms can escape from bubbles by irradiation-induced and thermal re-solution processes.

In the MFPR model, the FP release from the matrix is divided into two steps:

- Intragranular FP transport from the bulk to the grain boundary, accompanied by both formation of precipitates and gaseous species in the intergranular bubbles.
- Accumulation of gases in the intergranular bubbles, and release to open porosity through the system of bubbles and the grain boundaries and the network of channels and tunnels

Processes modeled by the MFPR code:

- a) Intragranular transport of FP elements:
 - Diffusion and release of chemically active FPs
 - Transport of fission gas
- b) Evolution of point defects in the irradiated fuel.
- c) Evolution of extended defects:
 - Pore evolution
 - Dislocation-loop evolution
- d) Evolution of intragranular gas bubbles
 - Intragranular bubbles under steady irradiation conditions at low temperatures $\leq 1500^{\circ}\text{C}$ (irradiation effects)
 - Intragranular bubbles under steady irradiation conditions at high temperatures $\geq 1500^{\circ}\text{C}$ (thermal effects)
 - Intragranular bubbles under transient conditions

- e) Intergranular FP transport, release and swelling models
 - Model of FP release by bubble interlinkage
 - Model for Xe grain-face diffusion transport
 - Intergranular-swelling process
- f) Fuel oxidation in steam/hydrogen mixtures

The principal phases that appeared in the irradiated fuel and considered in the code are the following:

- The fuel-FP oxide solid-solution: Cs(c), alkaline earth metals Ba(c) and Sr(c) and their oxides BaO(c), SrO(c), zirconium and niobium in the forms Zr(c), ZrO₂(c), Nb(c), NbO(c), NbO₂(c), rare earth elements La(c), Ce(c), Eu(c), Nd(c), and their oxides La₂O₃(c), Ce₂O₃(c), CeO₂(c), Eu₂O₃(c), EuO(c), Nd₂O₃(c), metalloid Sb(s) and Sb₂O₃(c), noble metals Mo(s), Ru(s) and their oxides MoO₂(c), RuO₂(c).
- The metal phase composed of Mo(c) and Ru(c).
- The phase of complex ternary-compounds (grey phase) including molybdates, zirconates and uranates of Ba, Sr and Cs in the form: BaUO₄(c), SrUO₄(c), Cs₂UO₄(c), BaMoO₄(c), SrMoO₄(c), Cs₂MoO₄(c), BaZrO₃(c), SrZrO₃(c) and Cs₂ZrO₃(c).
- The separate solid-phase of CsI(c).
- The gas phase with the main components: Xe(g), Te(g), I(g), Cs(g), CsI(g), Cs₂MoO₄(g), MoO₃(g), (MoO₃)₂(g), (MoO₃)₃(g), RuO(g), RuO₂(g), RuO₃(g), Ba(g), Sr(g), ZrO(g), LaO(g), CeO(g), NdO(g), NbO(g), O₂(g).

7. CONCLUSIONS

Currently, mechanistic models can simulate FP release from irradiated UO₂ fuel, as it is the case of the MFPR code. This code is based on self-consistent consideration of evolution of various point defects (gas atoms, vacancies and interstitials) and extended defects (gas bubbles, dislocations, vacancy clusters and pores) and their mutual interactions under various irradiation and annealing regimes of UO₂ fuel operation.

The main question is how to understand leaching experiments from the information obtain from mechanistic models in order to predict the Instant Release Fraction (IRF) from UO_2 fuels. As it is mentioned in Deliverable 4.2 [Pekala et al., 2013], IRF from the fuel requires the contact with water, therefore the release of these fission products would be related to the rate of wetting of the different parts of the fuel. Numerical modeling of fuel pellet saturation with water has been attempted as part of the First Nuclides project [Pekala et al., 2012].

Another interesting point is to know the behavior of the different compounds, showed above, when water contact the fuel. Solubilities of molybdates, zirconates and uranates and also of some oxides and metallic precipitates could allow to a general picture of the fast radionuclide release, combining both mechanistic models and leaching experiments.

8. REFERENCES

Carroll, D.F. J. Am. Ceram. Soc. 46 (1963) 195

Dehaut, P. (2000) Le combustible nucléaire et son état physico-chimique à la sortie des réacteurs. Rapport CEA-R-5923

González-Robles, E. (2011) Study of Radionuclide Release in commercial UO_2 Spent Nuclear Fuels. Effect of Burn-up and High Burn-up Structure. PhD Thesis, UPC-Barcelona Tech.

Gray, W.J. Inventories of I-129 and Cs-137 in the gaps and grain boundaries of LWR spent fuels. In *Scientific Basis for Nuclear Waste Management XXII*, (D. J. Wronkewicz and J.H. Lee, Editors), Mat. Res. Soc. Symp. Proc. 556 (1999) 487-494.

Heames, T.J. et al. VICTORIA: A Mechanistic Model of Radionuclide Behavior in the Reactor Coolant System Under Severe Accident Conditions, NUREG/CR-5545 SAND90-0756 Rev 1 R3, R4, 1992.

Hiernaut, J.-P., Wiss, T., Colle, J.-Y., Thiele, H., Walker, C.T., Goll, W., Konings, R.J.M. Fission product release and microstructure changes during laboratory annealing of a very high burn-up fuel specimen. J. Nucl. Mater. 377 (2008) 313–324.

Imoto, S. Chemical state of fission products in irradiated UO_2 . J. Nucl. Mater. 140 (1986) 19-27.

Johnson, L.H., Tait, J.C. (1997) Release of Segregated Radionuclides from Spent Fuel, SKB Technical Report 97-18.

Johnson, L.H., McGinnes, D.F. (2002) Partitioning of radionuclides in Swiss power reactor fuels. NAGRA Technical Report NTB 02-07.

Johnson L., Poinssot C., Ferry C. and Lovera P. (2004) Estimates of the instant release fraction for UO_2 and MOX fuel at $t=0$, in: A Report of the Spent Fuel Stability (SFS) Project of the 5th Euratom Framework Program, NAGRA Technical Report 04-08.

Johnson, L., Ferry, C., Poinssot, Ch., Lovera, P. Spent fuel radionuclide source-term model for assessing spent fuel performance in geological disposal. Part I: Assessment of the instant release fraction. J. Nucl. Mater. 346 (2005) 56–65.

Johnson, L., Günther-Leopold, I., Kobler Waldis, J., Linder, H.P., Low, J., Cui, D., Ekeroth, E., Spahiu, K., Evins L.Z. Rapid aqueous release of fission products from high burn-up LWR fuel: Experimental results and correlations with fission gas release. J. Nucl. Mater. 420 (2012) 54–62.

Kleykamp, H. The chemical state of the fission products in oxide fuels. J. Nucl. Mater. 131(1985) 221-246.

Kohli, R. The chemical state of fission products in LWR fuels related to long-term dry storage. in *Proceedings of a Workshop on the Chemical Reactivity of Oxide Fuel and Fission Products Release*. Berkeley (UK) April 1987

Kurosaki, K., Uno, M., Yamanaka, S. Chemical states of fission products in irradiated uranium-plutonium mixed oxide fuel. In Technology Reports of the Osaka University, 49 (1999) 29-35.

Nuclear Thermodynamic Database (NUCLEA) Version 2007-01, THERMODATA, 6, rue du Tour de l'Eau - 38400 Saint Martin d'Herès (F) 2007.

Matzke, H.J. Radiation enhanced diffusion in UO_2 and $(\text{U,Pu})\text{O}_2$. Radiation effects 75 (1983) 317-325.

Matzke, H.J. Atomic transport properties in UO_2 and mixed $(\text{U,Pu})\text{O}_2$. J. Chem. Soc. Faraday Trans. 2, 83 (1987) 1121-1142.

Matzke, H.J. Atomic mechanisms of mass transport in ceramic nuclear fuel materials. J. Chem. Soc. Faraday Trans. 8, 86 (1990) 1243-1256.

Matzke, H.J. Oxygen potential in the rim region of high burn-up UO_2 fuel. J. Nucl. Mater. 208(1994) 18-26.

Peehs, M., Manzel, R., Schweighofer, W., Haas, W., Haas, E., Würtz, R. On the behavior of cesium and iodine in light water reactor fuel rods. J. Nucl. Mater. 97 (1981) 157-164

Pekala, M., Riba, O., Duro, L. Models for fission products release from spent nuclear fuel and their applicability to the First Nuclides project. Deliverable (D-N^o:4.2) First Nuclide project 2013.

Pekala, M., Idiart A., Duro, L., Riba, O., Modelling of spent fuel saturation with water-approach preliminary results and potential implications. In *1st Annual Workshop Proceedings of the Collaborative Project "Fast / Instant Release of Safety Relevant Radionuclides from Spent Nuclear Fuel" (7th EC FP CP FIRST-Nuclides)*. Budapest (H), October 2012.

Poinssot, C., Toulhoat, P., Grouiller, J. P., Pavageau, J., Piron, J. P., Pelletier, M., Dehaut, P., Cappelaere, C., Limon, R., Desgranges, L., Jegou, C., Corbel, C., Maillard, S., Faure, M. H., Cicariello, J. C., Masson, M. (2001) Synthesis on the long term behavior of the spent nuclear fuel, Vol. I (ed. CEA).

Prussin, S.G., Olander, D.R., Lau, W.K., Hansson, L. Release of fission products (Xe, I, Te, Cs, Mo and Tc) from polycrystalline UO_2 . J. Nucl. Mater. 154 (1988) 25-33.

Rest, J., Zawadzki, S.A. FASTGRASS, A Mechanistic Model for the Prediction of Xe, I, Cs, Te, Ba and Sr release from Nuclear Fuel under Normal and Severe-Accident Conditions, NUREG/CR-5840 TI92 040783, 1994.

Roudil, D., Jégou, C., Broudic, V., Muzeau, B., Peugeot, S., Deschanel, X. Gap and grain boundaries inventories from pressurized water reactors spent fuels. J. Nucl. Mater. 362 (2007) 411-415.

Sari, C., Walker, C.T., Schumacher, G. Solubility and migration of fission product barium in oxide fuel. J. Nucl. Mater. 79 (1979) 255.

Schmid-Fetzera, R., Andersson, D., Chevalier, P.Y., Eleno, L., Fabrichnaya, O., Kattner, U.R., Sundman, B., Wang, C., Watson, A., Zabdyr, L., Zinkevich, M. Assessment techniques, database design and software facilities for thermodynamics and diffusion. *Computer Coupling of Phase Diagrams and Thermochemistry* 31 (2007) 38–52

Serrano-Purroy, D., Clarens, F., González-Robles, E., Glatz, J., Wegen, D., de Pablo, J., Casas, I., Giménez, J., Martínez-Esparza, A. Instant release fraction and matrix release of high burn-up UO₂ spent nuclear fuel: Effect of high burn-up structure and leaching solution composition. *J. Nucl. Mater.* 427 (2012) 249-258

Thomas, L. E., C.E.Beyer, Charlot, L. A. Microstructural analysis of LWR spent fuels at high burnup. *J. Nucl. Mater.* 188 (1992) 80-89.

Van Uffelen, P. The potential of TRANSURANUS code for source term calculations of spent. In *1st Annual Workshop Proceedings of the Collaborative Project "Fast / Instant Release of Safety Relevant Radionuclides from Spent Nuclear Fuel" (7th EC FP CP FIRST-Nuclides)*. Budapest (H), October 2012.

Veshchunov, M.S. , Ozrin, V.D., Shestak, V.E., Tarasov, V.I., Dubourg, R., Nicaise, G. Development of the mechanistic code MFPR for modeling fission-product release from irradiated UO₂ fuel. *Nuclear Engineering and Design* 236 (2006) 179–200.

(D-N°: 4.1) – STATUS OF MODELLING OF MIGRATION/RETENTION PROCESSES OF FISSION PRODUCTS IN THE SPENT FUEL STRUCTURE

Dissemination level: PU

Date of issue of this report: 5/5/2013

